



PCCP

On the electrostatic nature of electrides

Journal:	<i>Physical Chemistry Chemical Physics</i>
Manuscript ID:	CP-ART-04-2015-002112
Article Type:	Paper
Date Submitted by the Author:	11-Apr-2015
Complete List of Authors:	Kumar, Anmol; IIT Kanpur, Chemistry Gadre, Shridhar; IIT Kanpur, Chemistry

SCHOLARONE™
Manuscripts

Article

On the electrostatic nature of electriles

Cite this: DOI: xx.xxxx/xxxxxxx

Anmol Kumar^a and Shridhar R. Gadre^a

Received xxth January 2015,

Accepted xxth January 2015

DOI: xx.xxxx/xxxxxxx

www.rsc.org/

Abstract

The nature of electron localization in electriles is explored by examining their electrostatic features. *Ab initio* investigations of three experimentally synthesized and two theoretically modeled organic electriles are performed in order to unveil the characteristics of trapped electron and to understand the reason for their low thermal stability. Single molecular unit of electrile extracted from the crystal structure shows unusually deep minimum in its electrostatic potential, located far away from its van der Waals surface. A comparison of electrostatic features of the usual electron localization such as lone pairs has been drawn against those of the trapped electron in the crystal voids of electriles. Further characterization of the MESP minimum brings out the isotropic behavior of the trapped electrons as compared to the lone-pair minimum which is strongly directional. The analysis of single molecular behavior of electrile has been extended to the set of molecules in the unit cell of the crystal lattice. Present study also suggests the criteria for ligands to achieve thermally stable organic electriles.

Introduction:

Organic electriles are stoichiometric ionic solids comprising of repeating units of certain supramolecular complexants ligating alkali metal atoms in a crystal lattice. They are presumed to contain electrons, provided by the valence 's' orbital of the alkali metal atom, located in the crystal voids. Thus the alkali atom behaves as a cation,^{1,2} complexed by the ligands e.g. Cs⁺(15-crown-5)e⁻. Such trapped electron could neither be assigned to any atom/molecule nor it is free electron cloud as in metals. The ligating structure is responsible for separation of alkali metal cation from the trapped electron ensuring that they do not recombine.³ These semi-isolated electrons in the

voids endow the electriles with properties such as high magnetic susceptibility, high polarizability and very high reducing character.³ Most of the organic electriles are observed to possess one-dimensional chain of electron trapping cavities connected via narrow channels. This allows spin-spin antiferromagnetic coupling between adjacent electron trapping.³ An analogous phenomenon of electron localization in voids is also seen in crystal defects of alkali halides (such as KCl) also known as F-centers, wherein electrons are localized in anionic vacancies.

Pioneering and extensive work on synthesis and analysis of electriles has been carried out by Dye and coworkers. First crystalline electrile, *viz.* $\text{Cs}^+(18\text{-crown-6})\text{e}^-$ was synthesized⁴ in 1983 wherein the structure was speculated on the basis of its properties. Later, in 1986, Dye and coworkers determined¹ its crystal structure using X-ray diffraction. Such electriles fall under the category of organic electriles which generally possess very low thermal stability and are operational below -30°C . It was only in 2005 that a thermally stable organic electrile *viz.* $\text{Na}^+(\text{tri-pip-aza-2.2.2})\text{e}^-$ was synthesized by Redko *et al.*^{5,6} On the other hand, inorganic counterparts of electriles are known to be resilient towards high temperature. Matsuishi *et al.*⁷ synthesized a distinct inorganic electrile, *viz.* $[\text{Ca}_{24}\text{Al}_{28}\text{O}_{64}]^{4+}\cdot(4\text{e}^-)$ wherein only four out of twelve vacancies in the unit cell contain trapped electrons.

Very few attempts have been made to theoretically justify the intriguing behavior of electrons in electriles and factors governing their stability. Singh *et al.*⁸ performed self-consistent local density functional calculations on $\text{Cs}^+(15\text{-crown-5})\text{e}^-$ employing plane waves, for understanding their energy band distribution as well as electronic and magnetic behavior. The localization of electrons in the voids was interpreted by plotting the isosurfaces of density constructed using the wave functions at the center of the Brillouin zone. Although it was amusing to find the self-consistent potential to be repulsive in the cavities, the localization of electron in voids was justified by lowering of their kinetic energy. A similar attempt for understanding the behavior of all the known crystal geometries of electriles was recently carried out by Dale *et al.*⁹ Valence band densities obtained from plane wave/pseudopotential approach with periodic boundary condition were utilized by them to visualize the localized regions of electron density in the voids. A related study has been performed by Taylor *et al.*¹⁰ wherein microscopic structure of solvated electron in anionic water clusters has been explored through the topological analysis of electron density. When the present article was being submitted for publication, a work¹¹ reported the use of ELF and Laplacian of electron density to justify the existence and provide the characteristics of electrons in molecular electriles. It has attempted to generalize the category of molecules which may bear electrile like properties, distinctively the loosely held electron cloud, on the basis of their ELF and Laplacian values.

In the present article, we have performed electrostatic potential investigation of electriles on single molecular units as well as entire unit cell extracted from crystal structures of experimentally synthesized organic electriles. The scalar field of molecular electrostatic potential (MESP) and its topography has proved to be an invaluable tool¹²⁻¹⁹ for exploring the nature of electron localization in molecular systems. Extensive studies have been performed employing MESP on various molecules, anions and radical systems to gain insights into their

electronic distributions.¹⁷ A recent article¹⁸ has shown that it is possible even to differentiate between various kinds of electron localization such as lone pairs, aromatic clouds etc. by examining the eigenvalues and eigenvectors of the Hessian of three dimensional field of MESP. Thus, in addition to a detailed knowledge of electronic bands and their behavior in crystals obtained from previous DFT-based studies,^{8,9} a finer understanding of nature of electronic distribution in electriles demands a scrutiny through such a scalar field. In the present article, we explore the characteristics of trapped electron, including their comparison with lone pairs, and the reason for their low thermal stability. We have also highlighted the electrostatic behavior of supramolecular complexants and their role in attaining the trapped electron. Important features of molecular electron density (MED) and its topography are also briefly discussed in order to gain deeper insights into electronic behavior of some electriles.

Theory:

Pioneering works on the scalar field of MESP was reported¹² by Tomasi and Pullman who used MESP as a tool for locating the sites of electrophilic attack. The usage of MESP as a descriptor of various chemical properties such as bonding, chemical reactivity, etc. was carried on by Politzer *et al.*^{13,14} Later, extensive work on the quantification of MESP¹⁹ and exploring its applications in most of the chemical phenomena¹⁶ have been performed by Gadre and coworkers.

The MESP, $V(\mathbf{r})$ generated by a molecule at a point \mathbf{r} , is given by

$$V(\mathbf{r}) = \sum_A^N \frac{Z_A}{|\mathbf{r} - \mathbf{R}_A|} - \int \frac{\rho(\mathbf{r}') d^3r'}{|\mathbf{r} - \mathbf{r}'|} \quad (1)$$

where first term in Eq. (1) is the positive potential generated by N nuclei with nuclear charges $\{Z_A\}$, located at $\{\mathbf{R}_A\}$, while the second one is the negative potential created by continuous electron density, $\rho(\mathbf{r})$ centered at \mathbf{r} . As evident from Eq. (1), MESP can attain positive as well as negative values. The topographical features of MESP are quantitatively brought out in terms of its critical points denoted as (R, σ) , where R is the rank of the corresponding Hessian matrix, *viz.* and σ represents the sum of sign of the eigenvalues. A CP is said to be non-degenerate if all the eigenvalues are non-zero. The nondegenerate CP's bear chemical significance regarding bonds and electron localizations. A negative minimum in MESP, denoted as $(3, +3)$ CP, vividly brings out the electron localization. Additionally, the eigenvalues and eigenvectors of the Hessian at this CP allow one to characterize the nature of localization *viz.* directionality and connectivity. Based on these criteria, lone pairs have been recently defined and distinguished from the aromatic or hydridic electron localizations. A rapid change in the function (MESP) value, indicated by numerically large eigenvalues provide the highly directional nature of lone pairs in comparison to other pockets of localizations. The value of the MESP at the $(3, +3)$ lone pair CP has proved to be a marker of its strength and shows an excellent correlation with the interaction energies of various non-covalent interactions involving lone pair.^{17,18}

Although the scalar field of electron density fails to bring out the regions rich in electrons, the latter may be studied through the Laplacian, $L(\mathbf{r}) = \nabla^2\rho(\mathbf{r})$, of the charge density, as well as the electron localization function (ELF). A region with $\nabla^2\rho(\mathbf{r}) < 0$ shows the local concentration of electrons whereas $\nabla^2\rho(\mathbf{r}) > 0$ is indicative of depletion.²⁰ Although $L(\mathbf{r})$ provides a detailed description of electron concentration and depletion, its full topological analysis is formidable for large molecules. Popelier *et al.*²¹ have also pointed out the poor and inconsistent correlation of $L(\mathbf{r})$ values with the protonation abilities of the lone pairs regions. Another popular descriptor of electron rich regions among theoretical chemists is the electron localization function (ELF) introduced by Becke and Edgecombe.²² ELF has been currently in vogue for studying various bonding patterns, disposition of lone pairs and aromatic clouds. A local maximum in the ELF function provides the position and the volume of the basins are analysed for contribution of electrons to the pockets of electron localization. However, faithful mapping of the function to the VSEPR model is still being developed.²³ In contrast, the uniqueness of MESP lies in the fact that its topographical features are just rich enough to bring out chemically salient features, especially the electron rich regions. More detailed comparison of various scalar fields and their capacity to bring out electronic behaviours can be found in our recent article.¹⁸

Methodology:

The quantum chemical calculations in the present work are performed using Gaussian09 suite of programs²⁴ on three geometries obtained from crystal structures^{1,2,25–28} viz. $\text{Li}^+(\text{Cryptand-2.1.1})\text{e}^-$ $\text{Na}^+(\text{tri-pip-aza-2.2.2})\text{e}^-$ and $\text{K}^+(\text{Cryptand-2.2.2})\text{e}^-$ and also on two theoretically designed electrified,^{29,30} viz. $\text{Li}^+(\text{Calix[4]pyrrole})\text{e}^-$ and $\text{Na}^+(\text{Calix[4]pyrrole})\text{e}^-$. Mono-anionic complexants devoid of alkali metals have been subjected to similar *ab initio* investigation. In order to understand the local and global nature of the trapped electron, the whole unit cell geometry has also been examined through *ab initio* calculations. Since large concentrations of electrons are loosely held by the molecular framework in these systems, the calculations are done at varying levels of theory viz. HF, MP2 and DFT (B3LYP) employing 6-31++G(d, p) basis-set for examining the effect of electron correlation on the electronic distribution. Topographical analysis of MED and MESP is carried out using the density matrices obtained at corresponding quantum chemical level of theory. Rapid topography mapping Fortran code developed recently by Yeole *et al.*³¹ has been employed for calculating the MED and MESP at grid points. Underlying algorithm for the evaluation of MED and MESP is based on deformed atoms in molecules (DAM) procedure proposed by Rico and López *et al.*³² The latter invokes the partitioning of scalar field into atomic contributions for rapid and sufficiently accurate function- and gradient-calculation.

Results and Discussion:

The isolated molecular units of electriles are analyzed first in order to comprehend the individual molecular contribution of electrons and its additive nature in the crystal lattice. Analysis is based on the results obtained from MP2/6-31++G(d, p), as well as HF and B3LYP level of theory employing 6-31++G(d, p) basis-set. Table 1 provides the distances of MESP minima from the metal atom and the associated MESP values obtained at the above levels of theory. Figure 1 displays the negative MESP minimum, a signature of maximum electron localization, wrapped around by relatively smaller valued negative isosurface for the various electriles studied. The van der Waals surface of these electriles is textured by MESP values in the range -0.001 (blue) to 0.001 (red) a.u. to distinctively bring out the corresponding negative and positive regions.

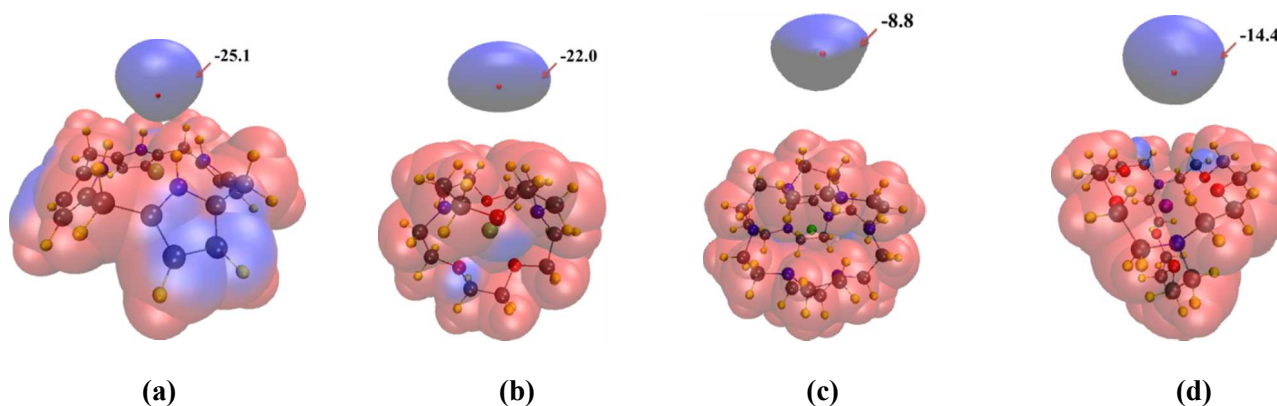


Figure 1. Negative MESP minima (red dots) enveloped by negative (blue) isosurfaces of indicated values (in kcal/mol), along with texturing of MP2/6-31++G(d,p) level MESP values [-0.001 (blue) to 0.001 (red) a.u.] on the van der Waals surfaces of (a) $\text{Li}^+(\text{Calix}[4]\text{pyrrole})\text{e}^-$ (b) $\text{Li}^+(\text{Cryptand-2.1.1})\text{e}^-$ (c) $\text{Na}^+(\text{tri-pip-aza-2.2.2})\text{e}^-$ and (d) $\text{K}^+(\text{Cryptand-2.2.2})\text{e}^-$. See text and Table 1 for details.

The unique feature emerging from Fig. 1 and Table 1 for electriles is the unusually distant localization of electron from the van der Waals surface of the molecular unit. Although the source of electron is the valence s-orbital of the alkali metal atom as indicated by previous studies,³ the distance between alkali atom and MESP minimum is typically greater than 3 Å for the experimentally investigated electrile. However, the two theoretically predicted electriles show relatively smaller separation. This engenders a physical picture that the ligand takes out the electron from the alkali metal by providing the required ionization potential and puts it into the void space. The large separation of electrons in the case of experimentally synthesized electriles (as compared to their theoretical counterparts) reflects that this distant electron localization is indeed a criterion for the stability of electriles. For example, $\text{Na}^+(\text{tri-pip-aza-2.2.2})\text{e}^-$, thermally most stable electrile obtained till now,⁵ shows the largest separation of electrons from the alkali atom. Consequently, large region of van der Waals surface of these molecules is seen to carry a positive potential except for the case of $\text{Li}^+(\text{Calix}[4]\text{pyrrole})\text{e}^-$ (theoretical electrile). The van der Waals surface of $\text{Na}^+(\text{tri-pip-aza-2.2.2})\text{e}^-$ is found to be entirely positive, thus creating a charge dipole (*cf.* Figure 1 (c)). Literature stresses on the complete encapsulation of the alkali metal by the supramolecular ligand for obtaining

isolation of electrons in the voids. The low thermal stability of the organic electriles has been attributed to reductive decomposition of the O-C ether linkage in crown ethers and cryptands with increase in temperature. The thermal stability of $\text{Na}^+(\text{tri-pip-aza-2.2.2})\text{e}^-$ is credited to its robust tertiary amine linkages. MESP analysis shows that the ability of complexant to push the electrons far away leads to screening of such linkages *viz.* ether and amine linkage, from the trapped electron.

Table 1. Locations and values of MESP minima in the isolated molecular units of electriles. Distances (D) from the respective alkali metal atoms in Å and MESP values (V) in kcal/mol. 6-31++G(d, p) basis-set used for all the calculations. See text for details.

	HF		B3LYP		MP2	
	D	V	D	V	D	V
$\text{Li}^+(\text{Calix}[4]\text{pyrrole})\text{e}^-$	1.7	-58.4	1.6	-36.8	1.6	-46.3
$\text{Na}^+(\text{Calix}[4]\text{pyrrole})\text{e}^-$	2.2	-58.0	2.1	-35.9	2.1	-45.7
$\text{Li}^+(\text{Cryptand-2.1.1})\text{e}^-$	3.5	-21.3	3.3	-9.0	3.3	-23.2
$\text{Na}^+(\text{tri-pip-aza-2.2.2})\text{e}^-$	8.5	-9.35	7.7	-2.0	8.5	-9.35
$\text{K}^+(\text{Cryptand-2.2.2})\text{e}^-$	6.9	-20.9	6.2	-5.2	6.0	-17.3

Another intriguing feature of electriles is the strength of these MESP minima. The MESP-derived point charges show that alkali metal atoms are positively charged, in spite of which the negative potential value at the (3,+3) CP in various electriles is found to be comparable to the MESP value associated to lone pair critical points. As evident from Table 1, the MESP derived at varying level of theory differs considerably. Hartree-Fock calculations lead to deepest MESP minimum, while the use of B3LYP functional numerically underestimates the same. MP2 results lie between these two extremes, closer to HF and are more reliable as the exchange and correlation interactions of electrons are proportionately treated. The theoretical electriles show unusually deep minima compared to those for the synthetic ones, leads to a stipulation that the strength of electron localization, is inversely related to stability of the electriles. As mentioned before, we have recently used the eigenvalues and respective eigenvectors of the Hessian matrix at the (3,+3) CP to define and differentiate lone pair electrons from delocalized electrons.¹⁸ In both the cases of lone pairs and delocalized π cloud, it was observed that one out of three eigenvalues is quite large than the other two, differing in the orders of magnitude. For example, the eigenvalues (all values in a.u.) of the CP associated to lone pair in H_2O molecule are 0.13, 0.03 and 0.006. This brings out the highly directional nature of these localizations. However, in the case of the CP associated with the trapped electron in $\text{Li}^+(\text{Calix}[4]\text{pyrrole})\text{e}^-$ and $\text{Li}^+(\text{Cryptand-2.1.1})\text{e}^-$, the eigenvalues (in a.u.) are (0.014, 0.012, 0.012) and (0.003, 0.001, 0.001) respectively. Comparable magnitude of these eigenvalues reveals the near-isotropic nature of these localizations as compared to lone pairs. In other words, such trapped electron can barely be associated with any specific atom in the nuclear framework. To summarize, the distant location, numerically small MESP values and isotropically distributed electron cloud for the molecular unit are favorable criteria for obtaining stable electriles.

Further, it is realized that the location of minima and its nature is actually determined by ligand structure rather than alkali metal atom. This conclusion emerges by analyzing the nature of MESP topography of mono-anionic ligating structure in absence of any alkali metal atom. It is observed that the location and nature of electron localization is almost similar to its electrone analog. The HOMO obtained from MO analysis for these anionic counterparts also shows similar disposition except in the regions encapsulated inside the cavity of complexants. Thus electron provided by alkali metal atom in LUMO of the neutral complexant largely dictates the MESP features of these systems.

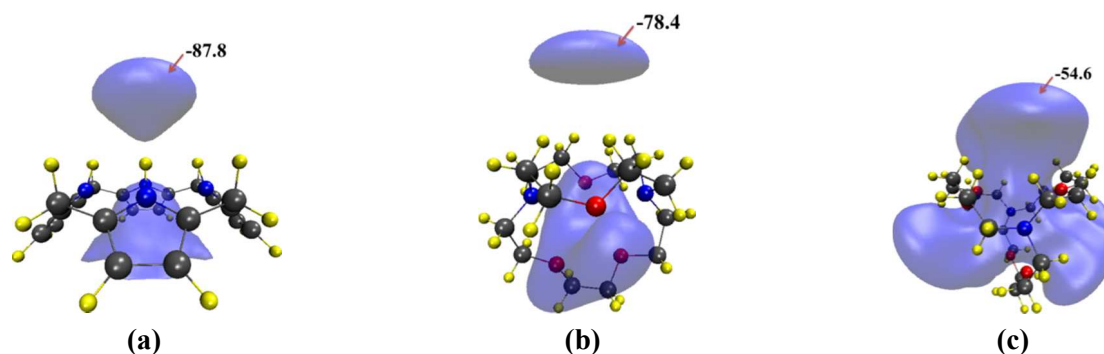


Figure 2. Negative MESP isosurfaces (with indicated values in kcal/mol) along with molecular unit of (a) [Calix[4]pyrrole][−] (b) [Cryptand-2.1.1][−] and (c) [Cryptand-2.2.2][−]. MESP values in (kcal/mol) generated using MP2/6-31++G(d, p) level of theory are indicated for corresponding complexants.

Figure 2 displays negative MESP isosurfaces for the anionic complexant structures. Electrostatically, it is intriguing to find a deep minimum located at such large distances from the anions. The separation of the negative regions for these anions remains roughly similar as in the electrone analogs. However, the values of these minima are deeply negative due to the absence of positively charged alkali metal atom. The cavity of these anions also bears large negative regions of potential which turn positive after complexation with the alkali atom. Figure 2 (c) depicts [Cryptand-2.2.2][−] which does not show distinct region of minima, because the negative potential created by lone pair electrons on oxygen and nitrogen atoms merge with distantly located negative regions. These analyses clearly indicate that the electronic properties of electrone are mainly governed by ligating structure rather than the alkali atom. Nonetheless, drastic increment in the negative values of MESP due to absence of positively charged alkali metal atom brings out the fact that a ligand able to ionize a particular alkali metal atom may form electrone and their qualitative properties will be almost independent of the alkali atom.

To figure out the reason behind the distant location of electron, the critical points of the corresponding molecular electron density (MED) are mapped. Interestingly, an infrequent feature of the presence of non-nuclear maxima^{16,33} is observed. These non-nuclear maxima are located in between the path joining alkali atom and MESP minima (see supplementary information). Such non-nuclear maxima in MED were first reported for Li and Na clusters by Cao *et al.*,³⁴ although they are scarce in complexes with single Li or Na atoms. An analysis of the same

reveals the fact that maximization of electron density occurs at certain location where MESP is completely positive. However, the negative MESP, being the cumulative effect produced by the electron density in a region of space and the nuclear potential, shows up at a farther distance.

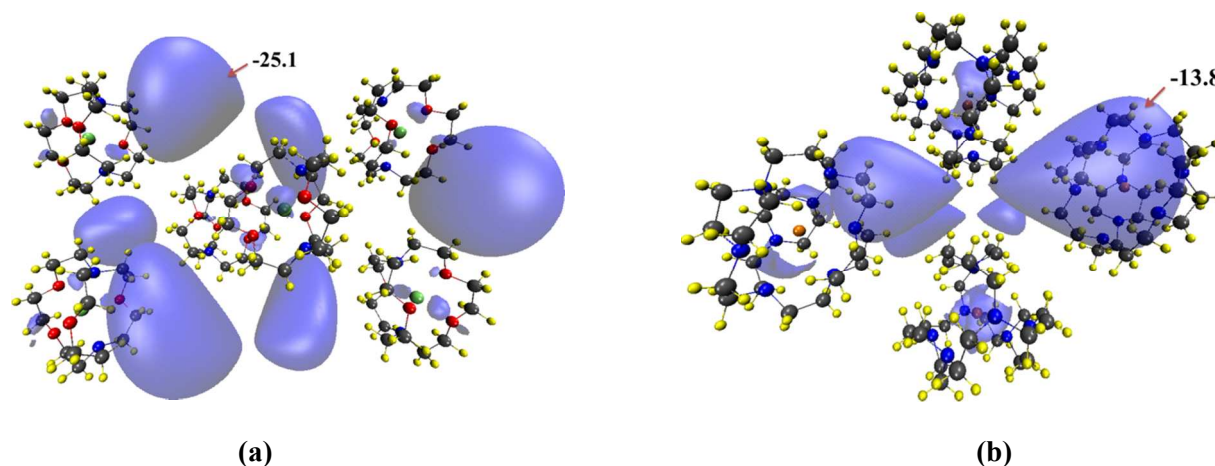


Figure 3. Negative-valued MESP isosurfaces of indicated values (in kcal/mol) in unit cell of (a) $\text{Li}^+(\text{Cryptand-2.1.1})\text{e}^-$ along c axis and (b) $\text{Na}^+(\text{tri-pip-aza-2.2.2})\text{e}^-$ along a axis, for a unit cell calculated at HF/6-31++G(d,p). See text for details.

Further, MESP analysis is extended for studying the behavior of electronegative species employing all the molecules occurring in its unit cell. Such analysis has earlier been carried out using plane waves/pseudopotential with periodic boundary conditions. Present work invokes quantum chemical investigation to probe the behavior of electrons in the voids of the crystal lattice. Different electronegative species are found to possess varying number of molecules in a unit cell of crystal lattice. Although it is expected that the properties at the boundaries of unit cell cannot be approximated well by studying just one unit cell, still the cumulative nature of electron localizations can be compared and correlated with the bulk property. *Ab initio* calculations at HF/6-31++G(d,p) level of theory, are employed to extract density profile of the unit cell. Higher level calculations are formidable given the large number of basis-functions involved. The density matrix thus obtained is employed to map the MESP features. Figure 3 provides the MESP isosurfaces along with the unit cell orientation along the ' c ' axis and ' a ' axis for $\text{Li}^+(\text{Cryptand-2.1.1})\text{e}^-$ and $\text{Na}^+(\text{tri-pip-aza-2.2.2})\text{e}^-$ respectively. $\text{Li}^+(\text{Cryptand-2.1.1})\text{e}^-$, comprising of six molecules in a unit cell, shows six distinct electron localization regions having the MESP value in the range of -44 to -54 kcal/mol, situated in crystal voids. On the other hand, $\text{Na}^+(\text{tri-pip-aza-2.2.2})\text{e}^-$ having four molecules in the unit cell, exhibits four regions of trapped electrons in the crystal voids, with the MESP value of ~ -19 kcal/mol. Comparing the values with single molecular unit at same level of theory indicates the cooperative effect of molecular units in enhancing the electron concentration in the crystal voids. The trapped electron is indeed found to reside at the locations of crystal voids, although the nature of the electron cloud is found to possess more anisotropy compared to those obtained from single molecular unit. Similar anisotropic nature of electron density has also been observed through DFT-based studies.

Conclusions

Electrostatic analysis of electrified surfaces reveals their unique and intriguing features. The distance of MESP minima from the van der Waals surface of electrified molecule is one such unusual feature which is also correlated to the stability of the electrified surface. Another interesting feature is brought out by texturing of MESP on the van der Waals surface, which shows that a large region of this surface carries a positive potential indicating the stability of electrified surfaces. The MESP values of the distantly located minima are unusually deep, almost comparable to lone pair electrons, in spite of the presence of positively charged alkali metal atom. The distribution of such electron localization is found to be quite isotropic, which implies that it may not be strongly associated with any atom in the molecular framework. Such electrostatic features endow the electrified surfaces with very strong reducing property. The nature and location of electron concentration is mainly governed by the type of the complexant whereas the alkali metal merely plays the role of providing the electron. Scrutiny of MESP features of the molecules within a unit cell indeed show the electrons to be trapped in the crystal voids and their MESP values are lowered drastically in the crystal due to the cooperative effect of molecular units. In summary, the present work sheds light on the nature of electron localization in experimental organic electrified surfaces, employing the tool of MESP, at both molecular level as well as in the unit cell, and highlighting further the aspect of their stability. It may be hoped that the molecular electrostatic potential offers a valuable tool for understanding and predicting the molecules for the development of future electrified surfaces.

AUTHOR INFORMATION

Corresponding Author

Professor Shridhar R. Gadre

Department of Chemistry,

IIT Kanpur, Kanpur – 208016, India

Email: gadre@iitk.ac.in

ACKNOWLEDGMENTS

A.K. thanks CSIR for a research fellowship. S.R.G. is thankful to the Department of Science and Technology (DST) for the award of the J. C. Bose National Fellowship.

Notes and references

^a Department of Chemistry, IIT Kanpur, Kanpur-208016, India.

Electronic Supplementary Information (ESI) available: [The variation of electrostatic potential and electron density away from the metal atom towards the MESP minimum.].

- 1 S. B. Dawes, D. L. Ward, R. H. Huang and J. L. Dye, *J. Am. Chem. Soc.*, 1986, **108**, 3534–3535.
- 2 S. B. Dawes, J. L. Eglin, K. J. Moeggenborg, J. Kim and J. L. Dye, *J. Am. Chem. Soc.*, 1991, **113**, 1605–1609.
- 3 J. L. Dye, *Acc. Chem. Res.*, 2009, **42**, 1564–1572.
- 4 A. Ellaboudy, J. L. Dye and P. B. Smith, *J. Am. Chem. Soc.*, 1983, **105**, 6490–6491.
- 5 M. Y. Redko, J. E. Jackson, R. H. Huang and J. L. Dye, *J. Am. Chem. Soc.*, 2005, **127**, 12416–12422.
- 6 M. E. Kuchenmeister and J. L. Dye, *J. Am. Chem. Soc.*, 1989, **111**, 935–938.
- 7 S. Matsuishi, Y. Toda, M. Miyakawa, K. Hayashi, T. Kamiya, M. Hirano, I. Tanaka and H. Hosono, *Science*, 2003, **301**, 626–629.
- 8 D. J. Singh, H. Krakauer, C. Haas and W. E. Pickett, *Nature*, 1993, **365**, 39–42.
- 9 S. G. Dale, A. Otero-de-la-Roza and E. R. Johnson, *Phys Chem Chem Phys*, 2014, **16**, 14584–14593.
- 10 A. Taylor, C. F. Matta and R. J. Boyd, *J. Chem. Theory Comput.*, 2007, **3**, 1054–1063.
- 11 V. Postils, M. Garcia-Borràs, M. Solà, J. M. Luis and E. Matito, *Chem. Commun.*, 2015, **51**, 4865–4868.
- 12 E. Scrocco and J. Tomasi, in *New Concepts II*, Springer Berlin Heidelberg, 1973, pp. 95–170.
- 13 P. Politzer and J. S. Murray, *Theor. Chem. Acc.*, 2002, **108**, 134–142.
- 14 P. Politzer, J. S. Murray and T. Clark, *Phys. Chem. Chem. Phys.*, 2010, **12**, 7748–7757.
- 15 S. R. Gadre and P. K. Bhadane, *J. Chem. Phys.*, 1997, **107**, 5625–5626.
- 16 R. K. Pathak and S. R. Gadre, *J. Chem. Phys.*, 1990, **93**, 1770–1773.
- 17 N. Mohan, C. H. Suresh, A. Kumar and S. R. Gadre, *Phys. Chem. Chem. Phys.*, 2013, **15**, 18401–18409.
- 18 A. Kumar, S. R. Gadre, N. Mohan and C. H. Suresh, *J. Phys. Chem. A*, 2013, **118**, 526–532.
- 19 P. Balanarayan and S. R. Gadre, *J. Chem. Phys.*, 2003, **119**, 5037–5043.
- 20 R. F. W. Bader, S. Johnson, T.-H. Tang and P. L. A. Popelier, *J. Phys. Chem.*, 1996, **100**, 15398–15415.
- 21 P. L. A. Popelier and P. J. Smith, *Phys. Chem. Chem. Phys.*, 2001, **3**, 4208–4212.
- 22 A. D. Becke and K. E. Edgecombe, *J. Chem. Phys.*, 1990, **92**, 5397–5403.
- 23 D. B. Chesnut, *J. Phys. Chem. A*, 2000, **104**, 11644–11650.
- 24 M. J. Frisch, G. W. Trucks, J. R. Cheeseman, G. Scalmani, M. Caricato, H. P. Hratchian, X. Li, V. Barone, J. Bloino, G. Zheng, T. Vreven, J. A. Montgomery, G. A. Petersson, G. E. Scuseria, H. B. Schlegel, H. Nakatsuji, A. F. Izmaylov, R. L. Martin, J. L. Sonnenberg, J. E. Peralta, J. J. Heyd, E. Brothers, F. Ogliaro, M. Bearpark, M. A. Robb, B. Mennucci, K. N. Kudin, V. N. Staroverov, R. Kobayashi, J. Normand, A. Rendell, R. Gomperts, V. G. Zakrzewski, M. Hada, M. Ehara, K. Toyota, R. Fukuda, J. Hasegawa, M. Ishida, T. Nakajima, Y. Honda, O. Kitao and H. Nakai, *Gaussian 09*, .
- 25 M. J. Wagner, R. H. Huang, J. L. Eglin and J. L. Dye, *Nature*, 1994, **368**, 726–729.
- 26 R. H. Huang, M. K. Faber, K. J. Moeggenborg, D. L. Ward and J. L. Dye, *Nature*, 1988, **331**, 599–601.
- 27 R. H. Huang, M. J. Wagner, D. J. Gilbert, K. A. Reidy-Cedergren, D. L. Ward, M. K. Faber and J. L. Dye, *J. Am. Chem. Soc.*, 1997, **119**, 3765–3772.
- 28 Q. Xie, R. H. Huang, A. S. Ichimura, R. C. Phillips, William P. Pratt and J. L. Dye, *J. Am. Chem. Soc.*, 2000, **122**, 6971–6978.
- 29 M. Garcia-Borràs, M. Solà, J. M. Luis and B. Kirtman, *J. Chem. Theory Comput.*, 2012, **8**, 2688–2697.
- 30 W. Chen, Z.-R. Li, D. Wu, Y. Li, C.-C. Sun and F. L. Gu, *J. Am. Chem. Soc.*, 2005, **127**, 10977–10981.
- 31 S. D. Yeole, R. López and S. R. Gadre, *J. Chem. Phys.*, 2012, **137**, 074116.
- 32 J. F. Rico, R. López, I. Ema and G. Ramirez, *J. Comput. Chem.*, 2004, **25**, 1347–1354.
- 33 G. I. Bersuker, C. Peng and J. E. Boggs, *J. Phys. Chem.*, 1993, **97**, 9323–9329.
- 34 W. L. Cao, C. Gatti, P. J. MacDougall and R. F. W. Bader, *Chem. Phys. Lett.*, 1987, **141**, 380–385.

